International Journal of Nanoelectronics and Materials
Volume 16 January 2023 [145-156]

New Comprehensive Stability and Sensitivity Analysis on Graphene Nanoribbon Interconnects Parameters

Zahra Zamini[1], Sevda Taheri[2], Babak Roshanipour[3,*], and Masoud Maboudi[4]

[1]Department of Electrical Engineering, Science and Research Branch, Islamic Azad University, Qazvin, Iran
[2]Department of Mathematics, Science and Research Branch, Payame Noor University
[3]East Azerbaijan Science and Technology Park, Atash Sakhtar Company
[4]Tabriz Machinery Manufacturing Company, Iran

Received 14 February 2022, Revised 4 July 2022, Accepted 20 July 2022

ABSTRACT

Based on the transmission line modeling for multilayer graphene nanoribbon (MGNR) interconnects, system stability was studied on intrinsic parameters. In addition to width, length and height variation, dielectric constant, permeability and Fermi velocity path change in multilayer graphene nanoribbon (MGNR) interconnects are analyzed. In this paper, the obtained results show with increasing dielectric constant and decreasing permeability, Fermi velocity system becomes more stable. Nyquist diagram and step response method results confirm these and are matched with physical parameter variation like resistance, capacitance and inductance in the following sensitivity analysis results where it shows with increasing width and length, sensitivity will decrease and increase respectively. Impulse response diagram results show with increasing 50% width, sensitivity will be zero but with increasing 50% length, amplitude will decrease and the time of setting will increase. On the other hand, from the step response of the transfer function, both width and length increase cause more stability for a system but the width parameter will be a better choice for manipulating the dimension of MGNR to reach a stable system.

Keywords: Multilayer graphene nanoribbon interconnects, Nyquist stability, step response, intrinsic feature, RLC model, sensitivity

1. INTRODUCTION

The role of graphene nanoribbon in the nanoelectronics industry is very prominent and many activities have been performed in this field. Length and width increase leads to a higher crosstalk voltage and the system becomes unstable. The graphene's superiority over the copper wires is kept even with the worst crosstalk [1]. Crosstalk effects on multilayer graphene stability have been investigated using time-domain response and Nyquist stability in Akbari and his colleague's research, where it is observed that the near-end output of the system together with both couplings is more stable and at its far-end output [2]. Modeling and simulation-based on carbon nanotubes and graphene nanoribbons for FET transistor [3] and stability analysis of multilayer graphene for the effect of switching on the noise voltage using the Nyquist method [4] are other researches in this field. Bandwidth variations and their impact on the stability of multilayer graphene using the Nichols method based on a new model which increases the length or decreases the width of the MGNRs, the stability increases in near-end output, and an increase in the length or width of MGNRs, stability decreases in far-end output [5]. A comparative study on their distributed parameters and transmission characteristics is performed in Wen-Sheng Zhao et al. paper. The transmission performance of the MGNR interconnects with different contacts is predicted and compared with their Cu and carbon nanotube counterparts at different technology nodes [6]. Chuan Xu et al. investigated the nanostructured multilayer graphene model and its

* b.roshanipour@gmail.com

analysis of zigzag distribution [7]. Problems in copper circuits can be solved by replacing carbon nanotubes, for example, where the carbon system has a higher heat-carrying capacity than the copper system because of its bundle [8]. By studying the structural properties of graphene, we have found that graphene is a material from a layer of carbon atoms with hexagonal structures, which is a two-dimensional lattice. Since the thickness of this carbon atoms sheet is only about the size of a carbon atom, it is considered to be a thin material [9]. Hafeng et al. investigated the physical properties of graphene and expressed the effect of adding nitrogen to the graphene structure, which graphene is used in energy and medicine, reducing pollutants and biotechnology [10]. Graphene optical interconnects for data centers which allow more interconnection between machines is another usage of graphene [11]. Manjit et al. investigated the impact of crosstalk on delay and the effect of crosstalk on the average power and noise of the multilayer graphene nanoribbon model [12, 13]. Nanorobots are very useful in the treatment of diseases, and the material of nano-robot used in this article is carbon [14].

In this paper, graphene stability criteria by the Nyquist diagram and step response method are investigated. Graphene communication lines can be used in industrial applications. Directly changing the intrinsic parameters of the communication lines such as the permeability, Fermi velocity and dielectric constant of the nano-ribbon is analyzed. Any of these changes will certainly affect the performance of graphene nanotubes used in the design of electronic circuits. Furthermore, achieving the optimum point in the nanoribbon stability will guarantee the best performance of the systems that used this technology. Also, the interaction between the mentioned intrinsic parameters is investigated. It is expected that with changes in physical parameters, relative stability change will be observed. In the meantime, the behavior of graphene communication lines will also change with changing parameters, and investigation on the sensitivity of graphene nanoribbon models is also conducted. Section 2 proposes a model of the system and the sensitivity algorithm, while in Section 3, results of the research is discussed, and ends with a conclusion in Section 4.

2. MATERIAL AND METHODS

The schematic shape of the multilayer graphene nanoribbon-based communication lines is shown from the front view in Figure 1.

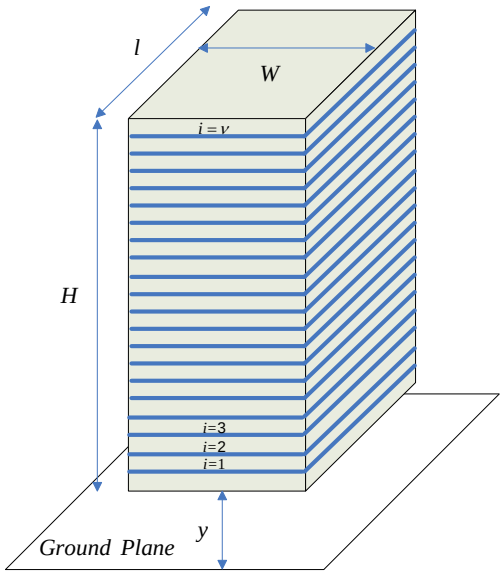

Figure 1. Schematic of graphene nanowire-based communication lines.

Figure **2** and
Figure **3** shows a distributed model of graphene nanoribbon.

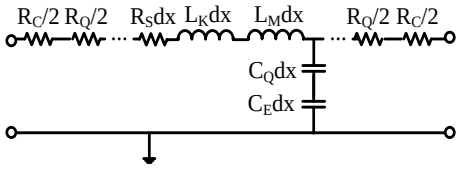

Figure 2. Typical RLC model for MGNR interconnects.

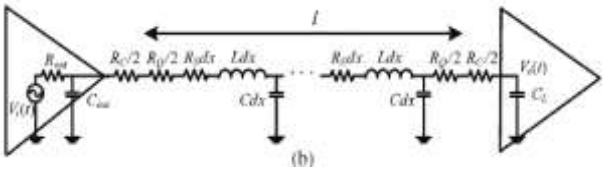

Figure 3. Transmission line circuit model for a driver-MGNR interconnect.

A typical RLC model for an MGNR interconnect made of N_{layer}, single GNR layers of the same lengths l and widths W are represented.$R_Q = {(\frac{h}{2e^2})}/{(N_{ch}\nu)} = {(\frac{h}{2e^2})}/{(N_{ch}N)}$is the minimum inherent resistance of quantum wire Planck's constant (h), and charge of electron (e). When the wire length larger than the electron effective mean free path ($\boldsymbol{\lambda}$), the distributed resistance (R_S) is introduced by electron scatting and can be written as $R_s = {R_Q}/{\lambda}$ [15].

$C_E \approx {\varepsilon W}/{d}$ and $L_M \approx {\mu d}/{W N_{layer}}$ are the length values of the equivalent capacitance per unit induced by the electrostatic effects and the magnetic inductance, in presence of the ground, in which e and μ are the dielectric permittivity in graphite and the graphene permeability (μ = 1) [16]. Furthermore, $L_K = {R_Q}/{v_F}$and $C_Q \approx \{R_Q v_F\}^{-1}$are kinetic inductance and quantum capacitance, respectively [17,18].

y, R_{out}, C_{out}, C_L , N_{ch}, υ, ν and v_F are height from earth, output resistance, output capacitance, load of capacitance, number of channels per layer, total available channels for carriers, layers of multilayer graphene nanoribbon, and Fermi velocity in graphite, respectively. Single layer graphene nanoribbon has high resistivity and the number of transmission channels is limited, so they increase the number of layers to reduce the resistance rather than increasing the bandwidth to achieve a higher channel number between the graphene nanoribbons.

In order to obtain the number of conducting channels in each GNR, one can add up contributions from all electrons in all conduction sub-bands and all holes in all valence sub-bands:

$$N_{ch} = \sum_{i=1}^{n_c}[1 + e^{{(E_{i,n}-E_F)}/{K_B T}}]^{-1} \qquad (1) + \sum_{i=1}^{n_V}[1 + e^{{(E_F-E_{i,h})}/{K_B T}}]^{-1} \qquad (1)$$

where E_F, K, T and $E_i = {ihv_F}/{2W}$ are Fermi energy, Boltzmann constant, temperature and the *quanti*energy that corresponds to the i_{th} conduction, respectively [19].

Taking advantage of the distributed nature of the interconnect into account, considering the interconnect as an *RLC* transmission line circuit model with perfect contacts ($R_C = 0$), and using the fourth-order Padé's approximation, the input–output transfer function becomes [20, 21].

$$H(S) = {}^{V_O(S)}/_{V_i}(S) \approx (\sum_{i=0}^{4} b_i s^i)^{-1} \quad (2)$$

All circuits have performance that varies as the value of the components change. Sensitivity importance is to choose the proper component selection and reach a stable system. Here, the change of transfer function in Equation (2) related to a specific component is investigated. [22,23]. The mathematical definition of sensitivity is as in Equation (3):

$$S_x^y = \lim_{\Delta x \to 0} \left\{ \frac{\frac{\Delta y}{y}}{\frac{\Delta x}{x}} \right\} = \frac{x}{y}\frac{dy}{dx} \quad (3)$$

where x is the variable and y is the transfer function.

According to Equation (3), we may interpret the sensitivity as the ratio of the little change in the circuit function y to the little change in the parameter x, provided that all changes are small enough (theoretically approaching zero). Sometimes we refer to S_x^y as the normalized sensitivity, in contrast with the unnormalized sensitivity, which is simply the partial derivative $\frac{dx}{dy}$.

Sensitivity studies are a basic step before calibration to identify the main parameters. One of the parameters is changed by a certain percentage, assuming the other parameters are constant. Sensitivity analysis can be applied to explore the robustness and accuracy of the model results under uncertain conditions.

If A is more sensitive than parameter B (meaning that the decision d is more sensitive to a unit change in parameter A than to a change in parameter B), so parameter A is more important than another one.

3. RESULTS AND DISCUSSION

According to the MGNR model, Nyquist stability and step response for dielectric constant, permeability, Fermi velocity, and mean free path are investigated. The parameter values are: W=10 nm, H=10 nm, y=100 nm, L=100 μm, EF=0.3eV, p=0, $Rout$=0 kΩ, $Cout$ =5fF and CL=5fF. For Nyquist stability analysis, the critical point of (−1, 0) in the complex plane must be outside of the Nyquist diagram for a stable system, and for step response, stable system become damper.

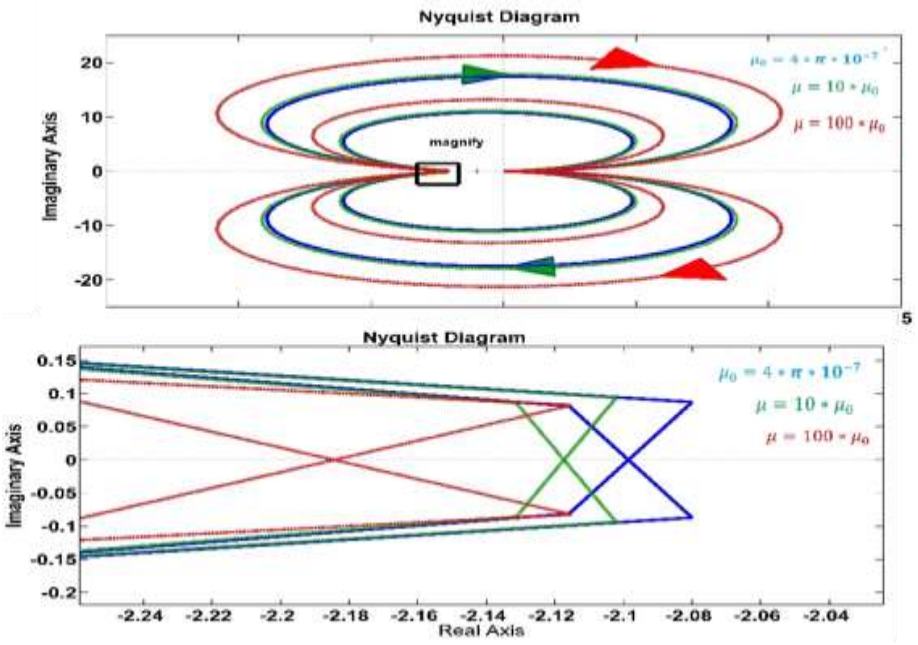

(a)

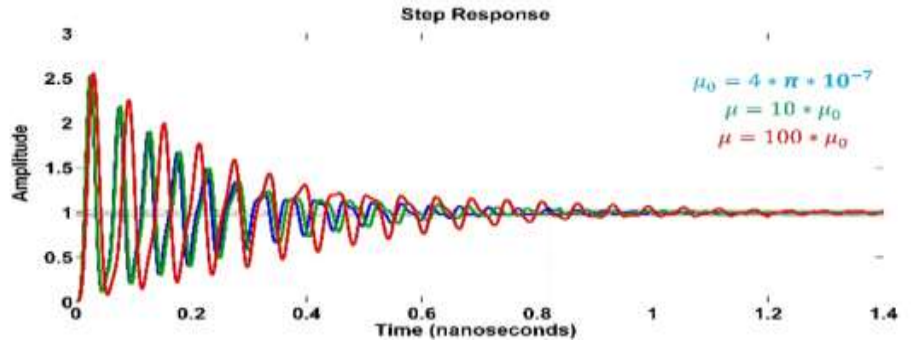

(b)

Figure 4. Permeability change for μ_0 , $10\mu_0$, $100\mu_0$ investigated in: (a) Nyquist stability analysis, (b) step response for MGNR model.

Figure 4 shows the effect of graphene nanoribbons permeability variation on the stability of the MGNR model. As shown in Figure 4(a), increasing amount of permeability system as it goes farther from the critical point (-1,0), means our system becomes unstable because in Nyquist diagram, critical point (-1,0) must be out of the diagram. In Figure 4(b), step response for ,10 and 100 indicate that our system become damper. For RLC circuit, damping ratio is $\zeta=\frac{R}{2}\sqrt{\frac{C}{L}}$ and $L=\mu d/WN_{layer}$ .with increasing, magnetic inductance increase and ζ decrease that means permeability (μ) effect on delay of system is undeniable.

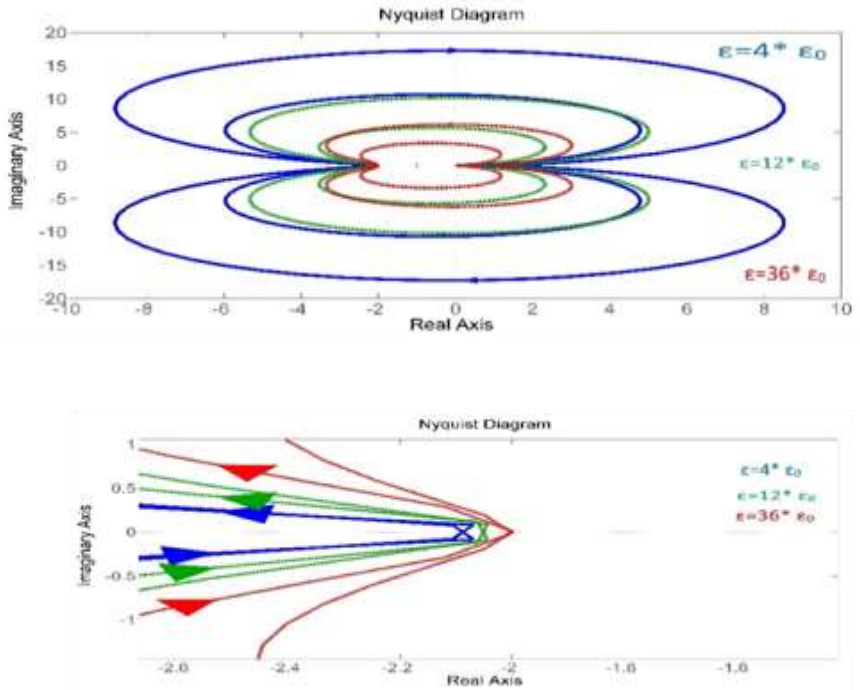

(a)

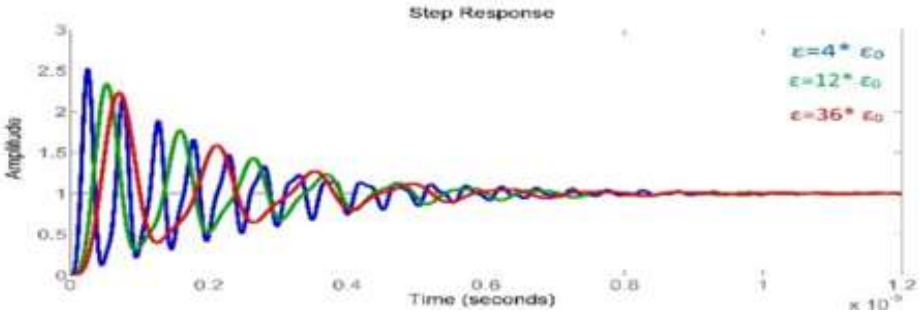

(b)

Figure 5. Dielectric constant change for $4 * \varepsilon_0$, $12 * \varepsilon_0$, $36 * \varepsilon_0$investigated in: (a) Nyquist stability analysis, (b) step response for MGNR model.

In

(a)

(b)

Figure 5, graphene nanoribbons dielectric constant (ε) change that effect on the stability of MGNR model is investigated.

(a)

(b)

Figure 5(a) shows, with increasing amount of dielectric constant system as it goes closer to a critical point (-1,0), our system becomes more stable because in Nyquist diagram critical point (-1,0) must be out of the diagram. In Figure 5(b), step response is shown that indicates our system with increasing become damper. For RLC circuit, damping ratio is $\zeta=\frac{R}{2}\sqrt{\frac{C}{L}}$ and $C=\varepsilon W/d$. With increasing ε, electrostatic capacitance of GNR increase and ζ increase, which means system will be more stable.

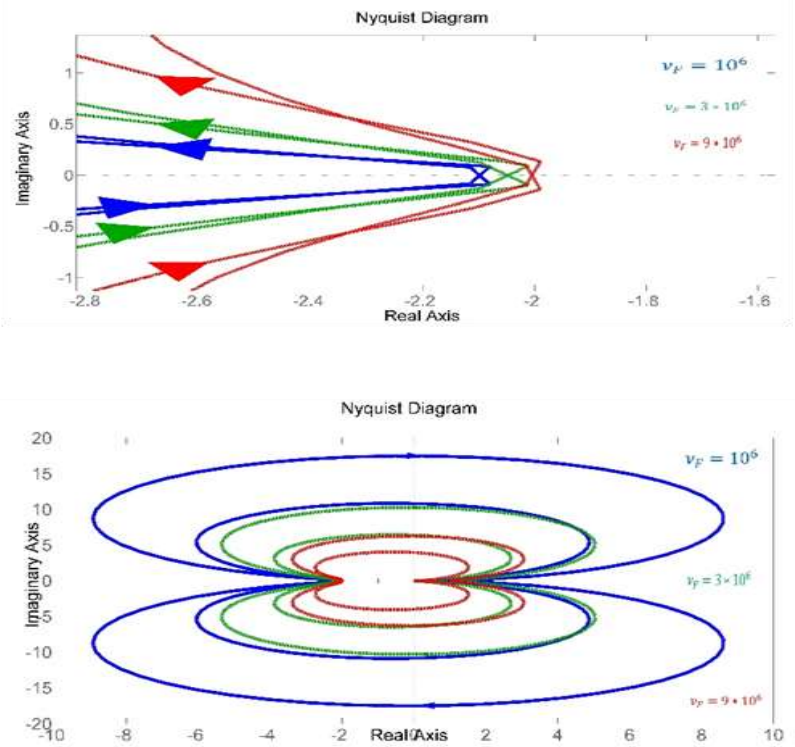

(a)

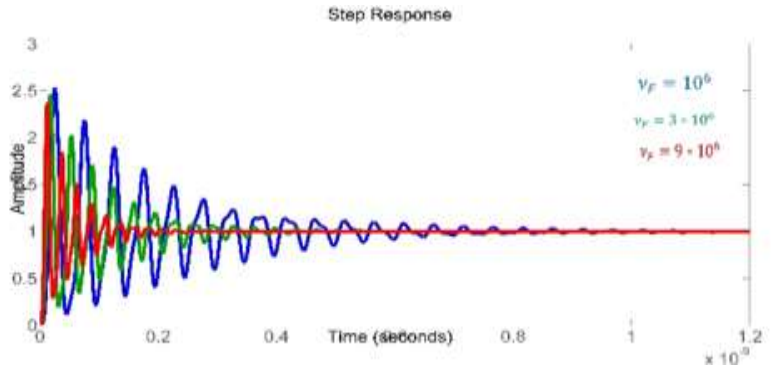

(b)

Figure 6. Fermi velocity (ν_F) change for 10^6, $3 * 10^6$, $9 * 10^6$ investigated in: (a) Nyquist stability analysis, (b) step response for MGNR model.

Figure 6 shows the effect of graphene nanoribbons while velocity (ν_F) variation on stability of MGNR model shown in **Error! Reference source not found.**(a) shows that with increasing amount of Fermi velocity, system goes farther from critical point (-1,0), which means our system become unstable because in Nyquist diagram critical point (-1,0) must be out of diagram. In (b), step response for 10^6, $3 * 10^6$, $9 * 10^6$ are shown which indicate our system with decreasing $v_F$become damper. For RLC circuit, damping ratio is $\zeta = \frac{R}{2}\sqrt{\frac{C}{L}}$ meanwhile $L_K = {}^{R_Q}/_{v_F}$ and $C_Q \approx \{R_Q v_F\}^{-1}$ are for kinetic inductance and quantum capacitance respectively. Meanwhile, Equation (4) shows:

$$C_{total} = {}^{(C_Q * C_E)}/_{(C_Q + C_E)} \text{ and } L_{total} = L_M + L_Q \quad (4)$$

With increasing v_F, C_Q and L_K decrease, so decreasing in C_{total} is more than L_{total} which caused decreasing ζ and system damping ratio decrease.

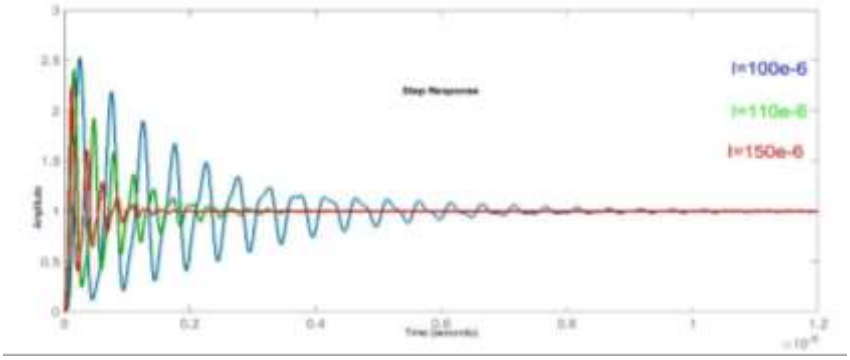

Figure 7. Step response for L=100e-6, L=110e-6, L=150e-6 for MGNR interconnects(W=100e-6).

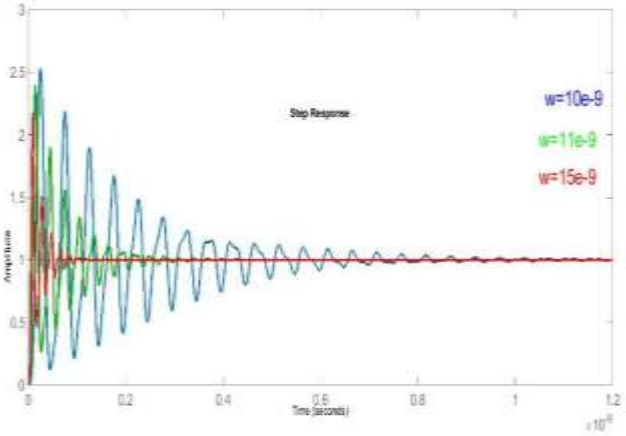

Figure 8. Step response for W=100e-6, W=110e-6, W=150e-6 for MGNR interconnects (L=100e-6).

As shown in
Figure **7** and Figure 8, with length and width increase, system stability increase. Step response in 10%, 50% variation were investigated, .in addition to system sensitivity analysis for L, W proposed. $S_L^{H(s)}$ *and* $S_W^{H(s)}$ are sensitivity of system transfer function on length and width of MGNR.

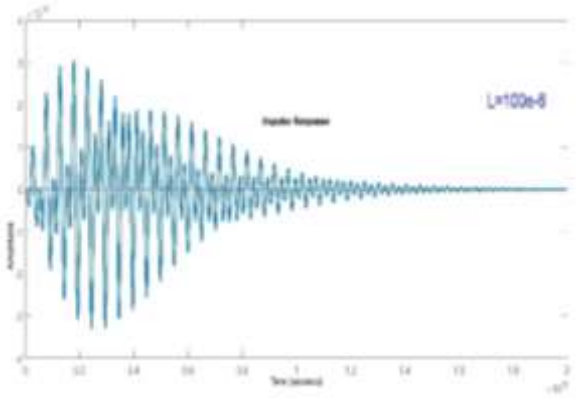

Figure 9. Impulse response for sensitivity of system on length with L=100e-6.

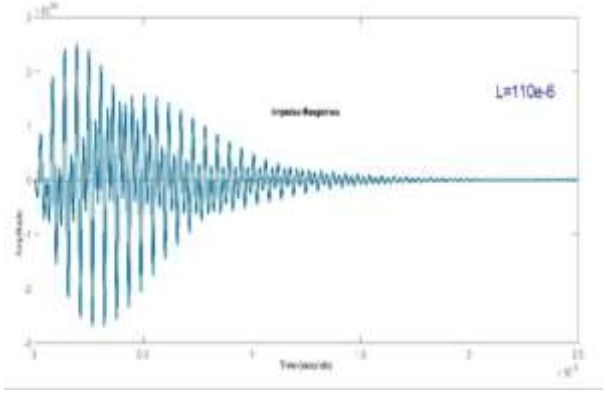

Figure 10. Impulse response for sensitivity of system on length with L=110e-6.

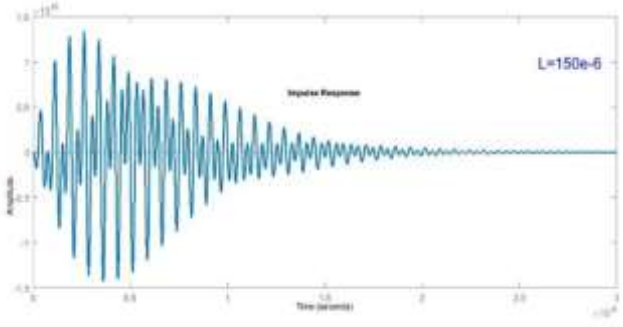

Figure 11. Impulse response for sensitivity of system on length with L=150e-6.

Figure **9**,
Figure **10** and
Figure **11** demonstrate changes in sensitivity with increasing length of system. With length increase, 10% and 50% amplitude of impulse function will decrease but time to reach zero will increase, that means sensitivity of the system to noise will increase.

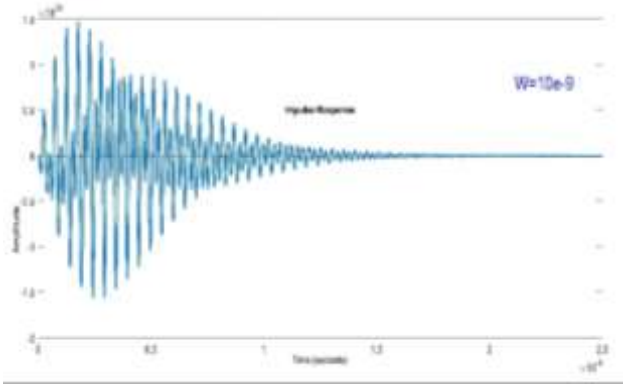

Figure 12. Impulse response for sensitivity of system on length with W=100e-9.

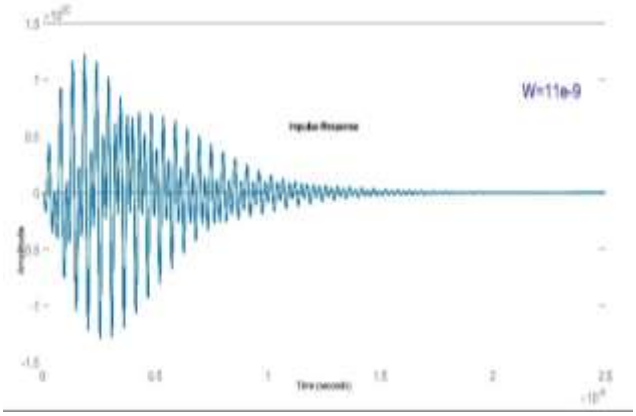

Figure 13. Impulse response for sensitivity of system on length with W=110e-9.

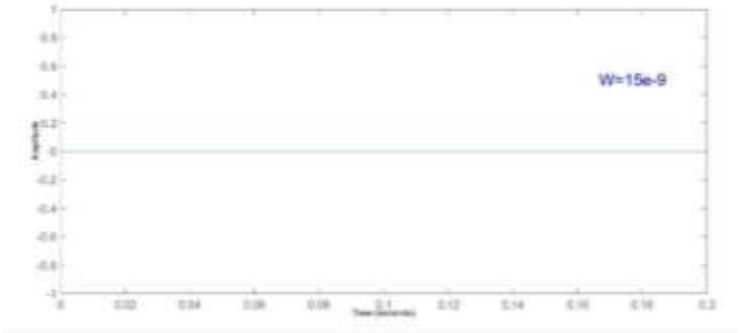

Figure 14. Impulse response for sensitivity of system on length with W=150e-9.

Figure 12, Figure 13 and Figure 14 demonstrate changes in sensitivity with increasing width of the system. With width increase, 10% and 50% amplitude of impulse function will decrease and time to reach zero will decrease, which means, sensitivity of the system to noise will decrease and will reach zero in 50% increase in width of the system.

When comparing impulse response of sensitivity for all the six-figures, this results can be earned: 1 – 10% and 50% increase in the amount of length and width reduces sensitivity; 2 – in 50% increase, sensitivity on width goes to zero; 3 – amplitude of sensitivity in transfer function on length variation goes to zero with the increase of length.

So, to reach a stable system with minimum sensitivity, manipulating width is a better choice against length.

4. CONCLUSION

Based on the transient model of graphene nanoribbon, stability of graphene nanoribbon using Nyquist and step response method are investigated and the result obtained, which is increasing dielectric constant and decreasing permeability and Fermi velocity caused increasing stability. In this paper, the effect of constant parameters is studied because changes in other parameters like length and width in some regions can make the system unstable. When changing these factors, the total system stability will upgrade and the application of graphene nanoribbons will be robust. Furthermore, sensitivity analysis on the width and length of the system is done and the result shows that the width of MGNR is comfortable to manipulate to reach a stable system. On the other hand, removing noise from the system by the width is very suitable and width parameter will be a better choice for manipulating the dimension of MGNR to reach a stable system. The main goal

of sensitivity analysis is to reach zero sensitivity for reducing the noise effect. Future research can discuss changes in intrinsic characteristics simultaneously with physical parameters like length and analyze their effect on each other with respect to system stability.

REFERENCES

[1] Pu, S. N., Yin, W. Y., Mao, J. F., Liu, Q. H.: Crosstalk prediction of single- and double-walled carbon-nanotube (SWCNT/DWCNT) bundle interconnects. IEEE Trans. Electron Devices 56(4), 560–568 (2009)

[2] International Technology Roadmap for Semiconductors (ITRS). 2011. (Available from: http://www.itrs.net/), Accessed Aug. 20, 2013.

[3] Sarto, M. S., Tamburrano, A.: Comparative analysis of TL models for multilayer graphene nanoribbon and multiwall carbon nanotube interconnects. In: Proceedings of IEEE International Symposium on Electromagnetic Compat, pp. 212–217. Fort Lauderdale (2010)

[4] Du X, Skachko I, Barker A and Andrei E 2008 Nature Nanotechnology 3 491{495 ISSN 1748-3387.

[5] McEuen P L, Fuhrer M S, Park H K. Single-walled carbon nanotube electronics. IEEE Trans Nanotechnol 2002;1(1):78–85.

[6] Xu C, Li H and Banerjee K 2009 IEEE Transactions on Electron Devices 56 1567{1578 ISSN 0018-9383

[7] Zhao W S, Yin W Y. Signal integrity analysis of graphene nano-ribbon (GNR) interconnects. In:2012 IEEE electrical design of advanced packaging and systems symposium (EDAPS); 2012. p. 227–30.

[8] L. Akbari, R. Faez, Crosstalk stability analysis in multilayer graphene nanoribbon interconnects, Circuits Syst. Signal Process. 32 (2013) 2653–2666.

[9] I. N. Hajj, On device modeling for circuit simulation with application to carbon nanotube and graphene nano-ribbon field effect transistor, IEEE Trans. Comput. Aided Des. Integr. Circuits Syst. 34 (3) (2015) 495–499.

[10] D. Libo Qian, Yinshui Xia, Shi Ge, Yidie Ye, Jian Wang “Stability analysis for coupled multilayer graphene nanoribbon interconnects,” Microelectronics Journal 58 (2016) 32–38.

[11] A. Amin Bagheri, Mahboubeh Ranjbar, Saeed Haji-Nasiri, Sattar Mirzakuchaki “Crosstalk bandwidth and stability analysis in graphene nanoribbon interconnects,”" Microelectronics Reliability (2015).

[12] W. S. Zhao, W. Y. Yin, Comparative study on multilayer graphene nano-ribbon (MGNR) interconnects, IEEE Trans. Electromagn. Compat. 56 (3) (2014)638–646.

[13] Xu C., Li H. and Banerji K., Aug. 2009, "Modeling, analysis, and design of graphene nano-ribbon interconnects," IEEE transaction on electron devices, Vol. 56, No. 8, pp. 1567-1578.

[14] Banerjee K., Srivastavan N., July 2006, "Are carbon nanotubes the future of VLSI interconnections," ACM Design Automation Conf. (DAC), CA, pp. 809–814.

[15] Geim A. K., Novoselov K. S., 2007, “The rise of graphene,” Nature Mat. Vol. 6, pp. 183-191.

[16] Haifeng Xuab, Lianbo Maa, Zhong Jina, 2018 ”Nitrogen-doped graphene: Synthesis, characterizations and energy applications” Journal of Energy Chemistry Volume 27, Issue 1, 1 January 2018, Pages 146-160.

[17] Manjit Kaur, Neena Gupta, Arun K. Singh. “Crosstalk analysis of coupled MGNR interconnects with different types of repeater insertion” Microprocessors and Microsystem Volume 67, June 2019, Pages 18-27.

[18] Cui, J. P., Zhao, W. S., Yin, W. Y.: Signal transmission analysis of multilayer graphene nano-ribbon (MGNR) interconnects. IEEE Trans. Electromag. Compat. 54(1), 126–132 (2012)

[19] Sandip Bhattacharya, Subhajit Das, Debaprasad Das “Analysis of Stability in Carbon Nanotube and Graphene Nanoribbon Interconnects” International Journal of Soft Computing and Engineering (IJSCE) ISSN: 2231-2307, Volume-2, Issue-6, January 2013.

[20] D. A. Areshkin, D. Gunlycke, C. T. White, Ballistic transport in graphene nanostrips in the presence of disorder: importance of edge effects, Nano Lett. 7 (1) (2007) 204–210.
[21] Y. W. Tan, Y. Zhang, K. Bolotin, Y. Zhao, S. Adam, E. H. Hwang, S. D. Sarma, H. L. Stormer, and P. Kim, "Measurement of scattering rate and minimum conductivity in graphene, Phys. Rev. Lett. 99 (24) (2007) 246803-1–246804-4.
[22] A. E. Schwarz, Computer-aided design of microelectronic circuits and systems, Academic Press, London, 1987.
[23] L. O. Chua, and P. M. Lin, Computer-Aided Analysis of Electronic Circuits: Algorithms and Computational Techniques, Englewood cliffs, NJ: Prentice-Hall, 1975.